Published in final edited form as:
Biotechnol Bioeng. 2011 May ; 108(5): 1119–1129. doi:10.1002/bit.23034.

Quantification of Both the Presence, and Oxidation State, of Mn in *Bacillus atrophaeus* Spores and its Imparting of Magnetic Susceptibility to the Spores

Jianxin Sun[1], **Maciej Zborowski**[2], and **Jeffrey J. Chalmers**[1]

Jeffrey J. Chalmers: Chalmers.1@osu.edu

[1]William G. Lowrie Department of Chemical and Biomolecular Engineering, The Ohio State University, 140 W 19th Ave, Columbus, Ohio 43210; telephone: +1-614-292-2727; fax: +1-614-292-3769

[2]Department of Biomedical Engineering, The Cleveland Clinic Foundation, Cleveland, Ohio

Abstract

Bacillus atrophaeus spores were previously reported to have significant magnetic susceptibility in a magnetic field due to the presence of Mn. However, relatively little is known about the total amount and distribution of the oxidation state of Mn associated with this specific strain's spores. Using the instrument, cell tracking velocimetry (CTV) both magnetically induced velocity and settling velocity was quantitatively measured. Visual observations, and calculated diameter using previously reported densities, indicate that the spores are present in the form of clusters of approximately 3–6 μm. Treatment of these clusters with EDTA or pH of 2.0 or below resulted in not only the disruption of the spore clusters, but also a significant decrease in magnetic susceptibility, in some cases by almost two orders of magnitude. Since the magnetic susceptibility of Mn varies significantly between the three typically reported valance states of Mn, Mn(II), Mn(III), and Mn(IV); X-Ray Photoelectron Spectroscopy, XPS, was used to determined the valance states of Mn in the spores. This XPS analysis, which penetrates up to 10 nm into the spore, returned the following fractions: 0.41, 0.38, and 0.21 for the valance states: Mn(II), Mn(III), and Mn(IV), respectively. The total mass of Mn associated with each spore cluster was determined by ICP-MS. A second, completely independent estimate of Mn mass associated with each spore cluster was made, by mathematically solving for the amount of Mn per spore cluster using the experimentally measured magnetophoretic mobility and the magnetic susceptibility of each of the valence states from the XPS analysis. IPC-MS returned a value of 3.28×10^{-11} g of Mn per spore cluster while the calculated estimation from mobility and XPS analysis retuned a value of 1.16×10^{-11} g, which given the complexity of the two techniques, is a reasonable agreement. Finally, a discussion of potential applications of the magnetic properties of these spores is presented.

Introduction

Bacillus atrophaeus, also called *Bacillus subtilis* var. *niger*, *Bacillus niger*, or earlier as *Bacillus globigii* (*bg*) is a rod-shaped, Gram-positive, aerobic and endospore forming bacterium. The shape may vary depending on growth conditions, but has typical dimensions of 0.5–1.0 μm wide by 2.0–4.0 μm long in the vegetative state (Nakamura, 1989). In the endospore state, a single spore of *B. atrophaeus* (ATCC #9372) is approximately 0.7 μm in width and 1.8 μm in length when measured in a dry state using advanced microscopic

Correspondence to: Jeffrey J. Chalmers, Chalmers.1@osu.edu.

techniques (Plomp et al., 2005). *Bacillus atrophaeus* is not as well studied as other *Bacilli*, such as *B. subtilis*, partially as a result of *B. atrophaeus* only becoming a new species in 1989 (Nakamura, 1989). Nakamura reports that the DNA relatedness of *B. atrophaeus* to *B. subtilis* ranges from 20% to 34%, and the G + C content is approximately 41–43%, determined by CsCl buoyant density. Further reclassifications have been conducted by analyzing 16s RNA (Fritze and Pukall, 2001) and amplified fragment length polymorphism (Burke et al., 2004). *B. atrophaeus* has routinely been used as a *B. anthracis* surrogate due to its lack of pathogenicity and unique colonial characteristics (Bargar et al., 2000). Thus, not only detection and separation of *Bacillus atrophaeus* has been studied, but also inactivation of the spores (Czerwieniec et al., 2005; Johnson et al., 2000; Lighthart et al., 2004; Saenz et al., 1999; Tobias et al., 2006).

Like iron, manganese (Mn) plays an important function in many biological systems. While there are a number of functions of manganese, a common occurrence is the association of Mn atoms with proteins involved in reduction-oxidation reactions. This is not surprising, given the various valence states of Mn, which has analogies to iron. Recently, significant interest has focused on the role of manganese superoxide dismutase (MnSOD, SOD2) in human pathological conditions. While a number of metal atoms can be present in superoxide dismutase, MnSOD has been shown to be an essential primary antioxidant enzyme in the mitochondrial matrix (Pardo-Andreu et al., 2006), and various forms occur in a wide range of organisms. In addition, the overexpression of MnSOD has been suggested to contribute to resistance of cancer cells to anti-cancer treatments such as radiation (Valdivia et al., 2009).

A number of bacteria, or spores of bacteria, can oxidize Mn, and at least one proposed mechanism is from the spores of the organism *Bacillus* sp. strain SG-1. This mechanism(s) have developed from the observation that different types of Mn oxides were found on the spore coat of B. sp. SG-1. For example, hausmannite (Mn_3O_4), deposited on spores of this marine strain, was reported by Hastings and Emerson (1986). Lattice imaging also revealed that amorphous deposits (Mn_3O_4) covered the spore coat in isolated domains (Mann et al., 1988). Moreover, Mn_3O_4 was deduced to be the intermediate in ultimate MnO_2 formation on the spores. Besides Mn_3O_4, Mn(IV) solid phase products were claimed to be formed in SG-1 oxidation via X-ray diffraction studies (Mandernack et al., 1995). In contrast to this hypothesis that Mn_3O_4 is an intermediate in a Mn oxidation pathway, Hem and Lind (1983) and Murray et al. (1985) observed that Mn(III) minerals only slowly aged to Mn(IV). A recent review article Spiro et al. (2010) reviews the current understanding of the presence of manganese oxides in a number of bacteria as well as summarize current thinking on the biological, manganese oxidation pathways.

Spore Aggregation

A number of different strains of *Bacillus* spores have been reported to form clusters in suspension (Burgos et al., 1972; Faris et al., 1997; Furukawa et al., 2005; Mamane-Gravetz and Linden, 2005; Sasaki et al., 1995). It was previously shown that different spore species possess different hydrophobic characteristics (Doyle, 2000; Flint et al., 2000; Koshikawa et al., 1989; Rosenberg, 1984), and it was suggested by Furukawa et al. (2005) that an increase of this hydrophobic characteristic can contribute to the formation of aggregations of these spores. While hydrophobicity and surface charge play a role in microbial surface adhesion, the magnitude of surface charge in increasing or decreasing the attachment of microbes to surfaces is not well understood (Flint et al., 2000). It should also be noted that a large body of literature exists that indicates that spores of *B. subtillis* and *B. anthracis* do not normally clump indicating the variety of states that spores can be observed.

Magnetic Properties

Like iron, manganese has paramagnetic properties, and these properties are a strong function of the oxidation state of the metal atom. Table I lists the compound, molecular weight, specific gravity, and magnetic susceptibility (in cgs units) of 1 g formula weight for the various, common forms of Mn and water (Weast et al., 1987). In addition to presenting magnetic susceptibility in the form of 1 g formula weight, χ_{molar}, it is also commonly presented as a volumetric magnetic susceptibility, χ; the two forms are related by:

$$\chi = \frac{\chi_m \rho}{M_w} \tag{1}$$

with M_w representing the molecular weight of the compound. This form of susceptibility is also presented in Table I, in the SI unit system.

Bulk Magnetic Susceptibility of a Mixture

Since it has been experimentally demonstrated that several strains of *Bacillus* spores can contain various forms of Mn, and, as is quantified in Table I, these various forms of Mn have significantly different values of magnetic susceptibility, one can apply the following relationship (Zborowski and Chalmers, 2007) to determine the weighted average value of the magnetic susceptibility of a *Bacillus* spore based on its composition:

$$\chi = \sum_{i=1}^{n} \varphi_i \chi_i = \frac{V_{\text{biomass}} \chi_{\text{biomass}} + V_{\text{Mn}} \chi_{\text{Mn}} + V_{\text{MnO}} \chi_{\text{MnO}} + V_{\text{Mno}_2} \chi_{\text{MnO}_2} + V_{\text{Mn}_2\text{O}_3} \chi_{\text{Mn}_2\text{O}_3} + V_{\text{Mn}_3\text{O}_4} \chi_{\text{Mn}_3\text{O}_4}}{V} \tag{2}$$

where φ_i is the volume fraction and χ_i is the volume magnetic susceptibility of species "*i*." It should be noted that Energy Dispersive spectroscopy, EDS, of several different strains of *Bacillus* spores (Melnik et al., 2007) indicates in addition to the basic atomic components of biomass present (i.e., Na, Ca, Mg, Al) Mn was present. However, the only other atom which is magnetic and typically found in biological samples, Fe, was not present (or at least below the EDS detection limits).

Relationships Defining Magnetic Susceptibility and Spore Diameter From Experimentally Determined Magnetically Induced Velocity and Settling Velocity

The magnetic force exerted on a volume, V, of a substance, characterized with a volumetric magnetic susceptibility, χ, is given by:

$$F = \chi \mathrm{V} \mathrm{H} \frac{\mathrm{d}B_0}{\mathrm{d}x} \tag{3}$$

where H and B_0 are magnitudes of the applied magnetic field vectors. One can define a magnetophoretic mobility, m, such that:

$$m = \frac{v_{\text{mag}}}{S_m} = \frac{v_{\text{mag}}}{\left| H \frac{\mathrm{d}B_0}{\mathrm{d}x} \right|} \tag{4}$$

And in the limiting case of a microsphere undergoing creeping flow,

$$m = \frac{v_{\text{mag}}}{\left| \frac{\nabla {B_0}^2}{2\mu_0} \right|} = \frac{(\chi_{\text{sphere}} - \chi_{\text{f}}) V_{\text{sphere}}}{3\pi D_{\text{sphere}} \eta} \tag{5}$$

where v_m is the magnetically induced velocity, S_m is the magnetic energy gradient (T-A/mm^2), B_0 is the magnetic field intensity (T), μ_0 is the permeability of free space (T-m/A), and χ_f is the magnetic susceptibility of the suspending buffer. Implicit in Equation (5) is the assumption that the sphere is linearly polarizable (either diamagnetic or paramagnetic).

In an analogous manner to a magnetically induced velocity, v_m, one can speak of a sphere's sedimentation velocity, v_g, which is the result of gravity acting on the differences in densities between the sphere and the suspending fluid:

$$s=\frac{v_g}{g}=\frac{(\rho_{\text{sphere}}-\rho_f)V_{\text{sphere}}}{3\pi D_{\text{sphere}}\eta} \tag{6}$$

Division of Equation (5) by Equation (6) (Jin et al., 2008) results in:

$$\frac{v_m}{v_g}=\frac{(\chi_{\text{sphere}}-\chi_f)}{(\rho_{\text{sphere}}-\rho_f)}\frac{S_m}{g} \tag{7}$$

Given the linear magnetic polarizability of manganese over the range of magnetic fields of the CTV instrument used in this study (0 to 1.2 T; Jin et al., 2008), Equation (7) indicates a linear correlation between v_m/v_g and S_m, with a slope defined by $\Delta\chi/g\Delta\rho$. Equation (7) can be further rearranged to solve for the magnetic susceptibility of a sphere:

$$\chi=\left(\frac{v_m}{v_g}\right)\frac{\Delta\rho g}{S_m}+\chi_f \tag{8}$$

In addition to determining the magnetic susceptibility of the sphere, the hydrodynamic diameter of the spheres can be determined from the settling velocity. Carrera et al. (2008) has reported the "wet" and "dry" densities of a number of *Bacillus* spores, including *Bacillus atrophaeus*. Using this experimentally determined value of density, the experimentally determined settling velocity from the CTV instrument (obtained in this study), and a rearrangement of Equation 6 (and the assumption of a perfect sphere $V_{\text{sphere}} = (1/6)\pi D^3$), the average diameter of the spores, or clumps of spores, can be determined from:

$$D_{\text{sphere}}=\left[v_g\frac{18\eta}{g\Delta\rho}\right]^{1/2} \tag{9}$$

Given this potential to measure the magnetic susceptibility of the spores, and various forms of Mn (Eq. 2) which imparts this magnetic susceptibility, we wish to further quantify both the amount of manganese, and the oxidation state, through the use of further analysis with complementary instrumentation and internal controls.

Materials and Methods

Strains and Sporulation

Bacillus atrophaeus (ATCC #9372) and *Bacillus* sp. SG-1 from *Bacillus* Genetic Stock Center at the Ohio State University were cultured in Mod G medium and sporulated using Mod G media as described before (Melnik et al., 2007). To create a greater amount of spores for a number of different analytical studies, the process was scaled up, using a Biostat B bioreactor with a working volume was 4 L, an aeration rate of approximately 2 L/min and an

agitation rate of 300 rpm. The pH was maintained at 7.45 during sporulation. The collected spores were freeze-dried and stored as dry powder for future analysis.

Mn Valence State Determination by X-Ray Photoelectron Spectroscopy

X-ray photoelectron spectroscopy (XPS) was used to quantify the valence state of Mn on the spore surface. XPS involves irradiating the surface of solid/powder sample in high vacuum, and subsequently measuring the kinetic energy of excited electrons from the atoms in the sample (Moulder, 1992). A limitation of this technique is that only the top 1–10 nm of the surface being interrogated is analyzed.

The lyophilized magnetic spores on carbon tape were used directly for XPS analysis. Al K-alpha X-ray was used as the X-ray source. For most samples and standards, such as Mn_3O_4, a charge of 2.3 eV was used to obtain a good background. For MnO_2, no neutralizer was applied. Since the spectrum created by this instrument results from X rays that can penetrate the sample to a depth of 1–10 nm, it was assumed that only information on the surface coating of the air dried spores was obtained. This instrument can typically detect elements with atom concentration above 0.1%.

Mn and Fe Concentration Determination by Inductively Coupled Plasma-Mass Spectroscopy (ICP-MS)

Ten milligrams of previously prepared, and desiccated, spores were suspended in deionized, distilled water, and separated into two aliquots. One sample was disrupted by sonication with intermittent treatments for 1 h until the sample appeared to be homogeneous; the other aliquot was maintained in an unaltered state. Both aliquots were subsequently dissolved using a modified CBD method (Neaman et al., 2004). These dissolved samples were then added to 20 mL of 0.3 M sodium citrate ($Na_3C_6H_5O_7$–$2H_2O$), 2.5 mL of 1 M sodium bicarbonate ($NaHCO_3$), 0.5 g of sodium dithionite ($Na_2S_2O_4$), and subsequently stirred for 1 h at 80°C (in a water bath). This spore lysate was then centrifuged and the supernatant portion was collected for ICP study. ICP measurements were made on a ThermoFinnigan Element2 Inductively Coupled Plasma Sector Field Mass Spectrometer.

Magnetophoretic Mobility, MM, of Treated Spores From Cell Tracking Velocimetry

As reported previously, Cell Tracking Velocimetry (CTV) was developed to quantify the m of cells and particles that have intrinsic magnetic susceptibility or that have been imparted this susceptibility through binding of antibody magnetic particle conjugates. CTV can measure the m of hundreds to thousands of cells (or particles) simultaneously, allowing significant populations sizes to be characterized (Chalmers et al., 1999; Moore et al., 2001; Zhang et al., 2005). The magnetically induced velocity of cells or particles can be determined by using the defined magnetic energy gradient, S_m, a microscope and CCD camera, and the associated software. By dividing the measured velocity by S_m, the m of the target entity, is obtained. S_m (approximately 142 T A/mm^2; Chalmers et al., 1999) is independent of microparticle position in the field of view using the permanent magnet version; alternatively, the magnitude of S_m can be varied with the electromagnet version (Jin et al., 2008). However, even though the value of S_m can vary based on current through the electromagnet, for a given current, the value of S_m is nearly constant in the field of view.

Results

Given the greater genetic and physiological information available for *Bacillus* species such as *B. subtilis*, *cerus*, and *thuringiensis*, ideally it would have been optimum if the quantification studies in this report were conducted on one of these three and not on the *Bacillus atrophaeus* spores. However, at the time this study was initiated, *Bacillus*

atrophaeus spores had the highest, and most consistent, magnetophoretic mobility. As we have continued investigating different strains of *Bacillus*, we have observed that one of the marine strains of *Bacillus*, *Bacillus sp SG-1*, can exhibit magnetophoretic mobilities of comparable values to *B. atrophaeus*. Future studies will include *Bacillus sp SG-1*.

Further, we observed variability in the magnetic susceptibility of the spores from spore formation run to run when conducted in 200 mL shake flasks. Given the significant difference in the magnetic susceptibility of Mn oxides, we questioned the reproducibility of the environmental conditions in shake flask cultures. In contrast, relatively constant magnetophoretic mobilities of the spores were obtained from five different runs using the 4 L bioreactors; mean mobility of 2.36×10^{-4} (mm^3/T A s; $n = 5$) standard deviation of 0.11×10^{-4} mm^3/A T s. In addition, we obtained, in general, in one 4 L bioreactor run, sufficient spores, approximately 55 mg dried, which allowed all of the analytical tests to be conducted from a single experimental run.

Magnetic Susceptibility Measurements of Polystyrene Microspheres, PSM

Given the quantitative focus of this work, we choose to measure the magnetic susceptibility of the spores with and without an internal "control;" consequently, we followed experimental protocols used in Chalmers et al. (2010). Specifically, diamagnetic, 15.3 μm (as reported by the manufacturer) polystyrene microspheres, PSM, were analyzed independently and, added to a suspension of the spore suspension prior to CTV analysis.

Figure 1A is a representative "dot" plot of only the PSM analyzed in the CTV system. The mean, one and three standard deviations for the settling velocity and magnetically induced velocity are presented as dashed lines in this figure. In addition to the dot plots, histograms of the two velocities are presented in 1B and 1C. The data for four independent analysis of these PSM is presented in Table II.

Using a diameter of 15.3 μm, an average, CTV measured settling velocity of 4.97×10^{-3} mm/s, a value of 9.8 m/s^2 for g, and a viscosity of 0.98×10^{-3} kg/m s, Equation (8) can be rearranged to solve for $\Delta\rho$:

$$\Delta\rho = u_g \frac{18\eta}{g D_{sphere}^2} = 39.0\ \mathrm{kg/m^3} \tag{10}$$

With this value of $\Delta\rho$, the value of the volumetric magnetic susceptibility, χ, for each PSM (or spores) can be determined using Equation (9).

With a value of S_m of 142 T A/mm^2 (1.42×10^8 N/m^3), a value of $\Delta\rho$ calculated from Equation (10), and a value of the magnetic susceptibility of water of -9.05×10^{-6}, the average value of the magnetic susceptibility of the PSM can be calculated and is presented in Table II. Four PSM samples and four mixtures of spores and PSM were independently analyzed using the CTV system equipped with the permanent magnet. For each sample, approximately 1,000 particles were tracked and the mean magnetic and settling velocity was determined. The mean, calculated magnetic susceptibility of the PSM in this study was -9.28×10^{-6} which is near the reported values for polystyrene (Watarai and Namba, 2001;) of -7.5×10^{-6} to -8.2×10^{-6}, and previous CTV measurements between −7.7 and -8.0×10^{-6} (Jin et al., 2008; Zhang et al., 2005).

Magnetic Susceptibility of Measurements/Calculations of the Spores

Figure 2 is a dot plot of a mix of the spores and the PSM previously above; also included is an enlarged view, with dotted lines representing the mean of the settling and magnetic

velocity and dashed lines representing three times the standard deviation from the previous CTV studies of PSM (i.e., Fig. 1).

Table II also presents the mean and standard deviations of the PSM and spores when analyzed as a mixture and subsequently partitioned into PSM and spore populations using the mean and standard deviation values for the PSM when evaluated independently. Comparing the mean magnetically induced velocity of the PSM by themselves and in the mixture with the spores shows a slight difference; however the difference is well within the standard deviations of the mean suggesting that the difference is not significant. Correspondingly, it is suggested that the values of the magnetically induced velocity and corresponding calculated values of the spore magnetic susceptibility (Eq. 7) is representative of the actual magnetic susceptibility of the spores. Based on this result, further analysis of the spores did not include the PSM controls.

In addition to the studies of mixtures of PSM and spores, four independent, CTV analysis were conducted on just the suspended spores. Figure 3A is a dot plot and histograms of the settling and magnetic velocity for one of these experiments. Unlike the PSM (Fig. 1), there is clearly a wide, non-normal distribution in the magnetic velocity of the spores, Figure 3B, and a much wider distribution in the settling velocity, Figure 3C. Significant clumping is present which can contribute to both the wider distribution in the settling velocity and the non-normal distribution in magnetic velocity. If one makes the assumption that the densities of the spores are uniform, and using the previously presented value of the spore density (Carrera et al., 2008) the diameter of the spore clusters can be determined using Equation (8) and are presented in Table II.

Treatment of Spores With pH and Chelating Agents

Given the large distribution in settling velocity, and the calculated, mean diameters which ranged from approximately 3 to 7 μm, we attempted to disaggregate the spores with various surfactants and or chelating agents. In addition, we tested incubating the spores in solutions of pH ranging from 5.0 to 0.6. These treatments had a variety of significant effects on both the aggregation and magnetic susceptibility of the spores.

Figure 4A and B is example of a dot plots of the spores prior to, and after treatment with EDTA in distilled water and Figure 5 is a dot plot after overnight treatment in a solution of pH 1.2. Visual inspections, and numbers provided in Table II indicate significant decrease in clumping and, corresponding, decrease in magnetic susceptibility for the EDTA and the low pH treated spores.

XPS Analysis of the Spores

Figure 6A is a representative plot of a XPS analysis of spores over the whole spectra, and Figure 6B is an enlargement over the binding energies associated with Mn oxides. To assist in the interpretation, and quantification of the spectra, in addition to the specific spores in this study, spectra for *B. cereus*, *B. sp SG-1*, and pure samples of Mn_2O_3, Mn_3O_4, MnO, and MnO_2 are included. Using the spectral deconvolution software, GRAM (Thermo Scientific, Philadelphia, PA) and the pure samples, the fraction contribution of each oxidation state of Mn to specific peaks was determined to be 0.41, 0.38, and 0.21 for Mn^{2+}, Mn^{3+}, and Mn^{4+}, respectively. Table III presents more information with respect to this analysis.

Quantitative Estimates of the Amount of Mn on the Spores

Using the average values of magnetic susceptibility of the spore clusters, the volume of these clusters calculated from the effective diameters of the spores (Table II), the volumetric

magnetic susceptibility of the various oxidation states of Mn, Equation (2) can be rewritten to obtain:

$$\chi_{\text{spore}} V_{\text{spore cluster}} = V_{\text{MnO}} \chi_{\text{MnO}} + V_{\text{MnO}_2} \chi_{\text{MnO}_2} + V_{\text{Mn}_2\text{O}_3} \chi_{\text{MN}_2\text{O}_3} + V_{\text{Mn}_3\text{O}_4} \chi_{\text{Mn}_3\text{O}_4} \quad (11)$$

Note the term corresponding to the magnetic susceptibility of the biomass was omitted as was the magnetic susceptibility of elemental Mn since only $MnSO_4$ was a constituent of the media. In these XPS studies we were only able to differentiate between Mn^{2+}, Mn^{3+}, and Mn^{4+}; we are not able to specifically quantify the presence of Mn_3O_4. Consequently, Equation (11) was further reduced to obtain:

$$\chi_{\text{spore clsuter}} V_{\text{spore cluster}} = V_{\text{Mn}^{2+}} \chi_{\text{Mn}^{2+}} + V_{\text{Mn}^{3+}} \chi_{\text{Mn}^{3+}} + V_{\text{Mn}^{4+}} \chi_{\text{Mn}^{4+}} \quad (12)$$

The values of χ for each oxidation state of manganese, Mn^{x+}, are listed in Table I, and the values of the volumes of corresponding Mn oxidation state, $V_{Mn^{x+}}$, can be determined from:

$$V_{\text{Mn}^{x+}} = (\text{mn mass in gram}) \left(\frac{\text{MW Mn}_x \text{O}_y}{\text{MW Mn}} \right) \frac{1}{\rho_{\text{Mn}_x O_y}} \left(\frac{1\ \text{m}}{100\ \text{cm}} \right)^3 \quad (13)$$

Using the values from Table I, the corresponding values of $V_{Mn^{2+}}$, $V_{Mn^{3+}}$, $V_{Mn^{3+}}$, are Mn Mass × 9.81×10^{-7}, Mn Mass × 1.2×10^{-7} and Mn Mass × 6.51×10^{-8}, respectively. Substituting these values for $V_{Mn^{2+}}$, $V_{Mn^{3+}}$, $V_{Mn^{3+}}$, the corresponding values of χ, and the product of $\chi_{\text{spore cluster}} V_{\text{spore cluster}}$ of 1.35×10^{-20}, into Equation (13), the value of Mn (weight) per spore cluster is determined to be 1.16×10^{-11} g.

Estimates of the Amount of Mn Per Spore

Independent experimental measurements, with respect to CTV and XPS analysis, of the amount of elemental Mn per spore were made using an inductively coupled Plasma-Mass Spectroscopy (ICP-OES MS) instrument. Table IV presents the results of the instrumental analysis as well as calculations with respect to the amount of Mn per spore cluster. While it not known why more Mn per spore cluster was observed in the non sonicated compared to the sonicated samples, 3.28×10^{-11} versus 1.96×10^{-11}, the general agreement with the estimated from CTV and XPS analysis obtained in the previous paragraph, 1.16×10^{-11} g Mn per spore cluster is encouraging. Further, the ICP-MS analysis with respect to low amount of Fe present further underscores the observation that the magnetic susceptibility is the result of Mn atoms.

Total Mn Mass Balance

For the batch of spores used in this study, a total of 55 mg of spores were produced in 4 L of mod G medium. From the ICP analysis (Table IV), there is 0.268 g of Mn per gram of spores; therefore, there is a total of 1.34 mg of Mn associated with all of the spores produced in that specific batch. Since the initial concentration of Mn in the mod G medium is 50 mg of $MnSO_4 \cdot 4H_2O$/L, a total of 4.48 mg Mn was available. Given a total of 1.34 mg of Mn was determined to be associated with the spores, the spores were able to collected 30% of the available Mn.

Discussion

As in our previous report, spores of *Bacillus atrophaeus* can have a significant, intrinsic, elevated paramagnetic susceptibility. However, in addition to merely equating the magnetic

susceptibility to the presence of Mn, in this study we were able to measure not only the amount of Mn per spore cluster, but also estimate the ratio of the different oxidation states of Mn. As noted above, some debate in the literature exists with respect to what oxidation states of Mn can be associated with the spores as well as the mechanism by which the Mn is oxidized. Cleary, the XPS analysis in this study demonstrates that the three typical oxidation/valance states, Mn^{2+}, Mn^{3+}, and Mn^{4+} are present in *Bacillus atrophaeus*, but only Mn^{2+} was introduced in the sporulation media.

The general agreement between the two, independent experimental approaches (ICP-MS and CTV/XPS) to estimate the number of grams of Mn per spore cluster, suggests that biologically relevant amounts of Mn can be detected and measured in biological entities if the valance state of the Mn is known. Conversely, if the total amount of Mn is known, CTV measurements of the magnetically induced velocity can be used to make estimates of the valence state of atoms. For example, Zborowski et al. (2003), reported the able to quantify the difference in the magnetophoretic mobility between oxygenated and deoxygenated red blood cells and demonstrate that this difference is consistent with theoretical calculations in the difference between oxygenated and deoxygenated hemoglobin. This difference in oxygenated and deoxygenated hemoglobin corresponds to the valance state of the iron.

The amount of Mn per spore cluster in this study is actually relatively high compared to previous reports on the amounts of iron per cell that has been estimated using the CTV instrument. For example, the iron content in a typical, single adult red blood cell is on the order of 1.3×10^{-13} g. More recently, Chalmers et al. (2010) reported that the CTV instrument can quantify the motion of the 1 μm, dextran iron oxide particles from Stem Cell Technology (Chalmers et al., 2010). The iron content of these 1 μm particles is approximately 3.4×10^{-13} g. In addition, the CTV instrument can detect on the order of 700, non-specifically bound MACS particles (Miltenyi Biotech, Inc., Auburn, CA) to a single cell. Using the magnetically induced velocity of the cell with these non-specifically bound MACS beads, and the assumption that Fe is in the from of Fe_3O_4, the amount of iron associated with each of these cells with non-specifically bound MACS particles is on the order of 5×10^{-15} g.

The significant drop in magnetic susceptibility of the spore cluster with low pH or EDTA (Figs. 4 and 5), and the corresponding decrease in cluster size, is consistent with the general observation in the literature that the Mn oxides concentrate on the outside surfaces of *bacillus* spores. Given the limitation of XPS spectroscopy to only provide information up to a penetration of only 10 nm, it is possible that deeper layers within the spore coating have different ratios of Mn oxides. This lack of penetration of XPS could also explain why the agreement of the amount of Mn per spore cluster using ICP-MS is not closer to the estimate from the CTV and XPS measurements.

A number of potential applications can be envisioned with the use of these magnetic spore clusters, including a surrogate for food pathogens and a scavenger for contaminating heavy metals. The relative high intrinsic magnetic susceptibility of these spores introduces the concept that they can be used to determine if a sterilization process adequately destroys spores. Spiro et al., 2010, in addition to reviewing Mn oxides and bacteria, summarized the ability of Mn(IV) to bind environmental contaminates such as Pb(II) and Zn(II). The combination of the high magnetic susceptibility and the heavy metal adsorption capabilities of these spores present the possibility of the use of the spores and a magnetic separation system, such are our previously reported continuous flow through system (Sun et al., 1998), to develop system to clean contaminated bodies of water.

From a more fundamental, mechanistic perspective, the general agreement in the various analytical techniques, and theoretical considerations, suggest that this analysis approach could be used to further address, or at least assist, in the studies, and debate in the literature, of the pathways by which Mn is oxidized in *Bacillus* spores. For example, it is conceivable that time course studies could be conducted on spore suspension, using the combination of CTV and XPS measurements outlined above, to develop kinetic relationships of the oxidation process of Mn.

Acknowledgments

This study was supported by the National Science Foundation (BES-0124897 to J.J.C.) and the National Cancer Institute (R01 CA62349 to M.Z.).

Contract grant sponsor: National Science Foundation

Contract grant number: BES-0124897

Contract grant sponsor: National Cancer Institute

Contract grant number: R01 CA62349

References

Bargar JR, Tebo BM, Villinski JE. In situ characterization of Mn(II) oxidation by spores of the marine *Bacillus* sp strain SG-1. Geochim Cosmochim Acta. 2000; 64(16):2775–2778.

Burgos J, Ordonex JA, Sala F. Effect of ultransonic waves on the heat resistance of *Bacillus cerus* and *Bacillus licheniformis* spores. Appl Microbiol. 1972; 24:497–498. [PubMed: 4627969]

Burke SA, Wright JD, Robinson MK, Bronk BV, Warren RL. Detection of molecular diversity in *Bacillus atrophaeus* by amplified fragment length polymorphism analysis. Appl Environ Microbiol. 2004; 70:2786–2790. [PubMed: 15128533]

Carrera M, Zandomeni RO, Sagripanti JL. Wet and dry density of *Bacillus anthracis* and other *Bacillus* species. J Appl Microbiol. 2008; 105(1):68–77. [PubMed: 18298528]

Chalmers JJ, Zhao Y, Nakamura M, Melnik K, Lasky L, Moore L, Zborowski M. An instrument to determine the magnetophoretic mobility of paramagnetic particles and labeled, biological cells. J Magn Magn Mater. 1999; 194:231–241.

Chalmers JJ, Xiong Y, Jin X, Shao M, Tong X, Farag S, Zborowski M. Quantification of non-specific binding of magnetic micro- and nano-particles using cell tracking velocimetry: Implication for magnetic cell separation and detection. Biotechnol Bioeng. 2010; 105(6):1078–1093. [PubMed: 20014141]

Czerwieniec GA, Russell SC, Tobias HJ, Pitesky ME, Fergenson DP, Steele P, Srivastava A, Horn JM, Frank M, Gard EE, Lebrilla CB. Stable isotope labeling of entire *Bacillus atrophaeus* spores and vegetative cells using bioaerosol mass spectrometry. Anal Chem. 2005; 77:1081–1087. [PubMed: 15858989]

Doyle RJ. Contribution of the hydrophobic effect to microbial infection. Microbes Infect. 2000; 2(4): 391–400. [PubMed: 10817641]

Faris GW, Copleand RA, Mortelmans K, Bronk BV. Spectrally resovled absolute fluorescence cross sections for bacillus spores. Appl Opt. 1997; 36:958–967. [PubMed: 18250761]

Flint SH, Brooks JD, Bremer PJ. Properties of the stainless steel substrate, influencing the adhesion of thermo-resistant streptococci. J Food Eng. 2000; 43(4):235–242.

Fritze D, Pukall R. Reclassification of bioindicator strains *Bacillus subtilis* DSM 675 and *Bacillus subtilis* DSM 2277 as *Bacillus atrophaeus*. Int J Sys Evol Microbiol. 2001; 51:35–37.

Furukawa S, Narisawa N, Watanabe T, Kawarai T, Myozen K, Okazaki S, Ogihara H, Yamasaki M. Formation of the spore clumps during heat treatment increases the heat resistance of bacterial spores. Int J Food Microbiol. 2005; 102(1):107–111. [PubMed: 15925006]

Hastings D, Emerson S. Oxidation of manganese by spores of a marine bacillus—Kinetic and thermodynamic considerations. Geochim Cosmochim Acta. 1986; 50(8):1819–1824.

Hem JD, Lind CJ. Nonequilibrium models for predicting forms of precipitated manganese oxides. Geoch Cosmoch Acta. 1983; 47:2037–2046.

Jin X, Zhao Y, Richardson A, Moore L, Williams PS, Zborowski M, Chalmers JJ. Differences in magnetically induced motion of diamagnetic, paramagnetic, and superparamagnetic microparticles detected by cell tracking velocimetry. Analyst. 2008; 133(12):1767–1775. [PubMed: 19082082]

Johnson YA, Nagpal M, Krahmer MT, Fox KF, Fox A. Precise molecular weight determination of PCR products of the rRNA intergenic spacer region using electrospray quadrupole mass spectrometry for differentiation of *B. subtilis* and *B. atrophaeus*, closely related species of bacilli. J Microbiol Methods. 2000; 40:241–254. [PubMed: 10802141]

Koshikawa T, Yamazaki M, Yoshimi M, Ogawa S, Yamada A, Watabe K, Torii M. Surface hydrophobicity of spores of *Bacillus* spp. J Gen Microbiol. 1989; 135:2717–2722. [PubMed: 2517297]

Lighthart B, Prier K, Bromenshenk JJ. Detection of aerosolized bacterial spores (*Bacillus atrophaeus*) using free-flying honey bees (Hymenoptera: Apidae) as collectors. Aerobiologia. 2004; 20:3–4.

Mamane-Gravetz H, Linden KG. Relationship between physiochemical properties, aggregation and u.v. inactivation of isolated indigenous spores in water. J Appl Microbiol. 2005; 98(2):351–363. [PubMed: 15659190]

Mandernack KW, Post J, Tebo BM. Manganese mineral formation by bacterial spores of the marine Bacillus strain SG-1: Evidence for the direct oxidation of Mn(II) to Mn(IV). Geochim Cosmochim Acta. 1995; 59:4393–4408.

Mann S, Sparks NHC, Scott GHE, De-Vrind-De Jong EW. Oxidation of manganese and formation of Mn_3O_4 (Hausmannite) by spore coats of a marine *Bacillus* sp. Appl Environ Microbiol. 1988; 54:2140–2143. [PubMed: 16347723]

Melnik K, Sun J, Fleischman A, Roy S, Zborowski M, Chalmers JJ. Quantification of magnetic susceptibility in several strains of Bacillus spores: Implications for separation and detection. Biotechnol Bioeng. 2007; 98(1):186–192. [PubMed: 17335063]

Moore LR, Rodrigues AR, Williams PS, McCloskey K, Bolwell BJ, Nakamura M, Chalmers JJ, Zborowski M. Progenitor cell isolation with a high-capacity quadrupole magnetic flow sorter. J Magn Magn Mater. 2001; 225(1–2):277–284.

Moulder, JF. Handbook of X-ray photoelectron spectroscopy. 1992.

Murray JW, Dillard JG, Giovanoli R, Moers H, Stumm W. Oxidation of Mn(II): Initial mineralogy, oxidation state and aging. Geochim Cosmochim Acta. 1985; 49:463–470.

Nakamura LK. Taxonomic relationship of black-pigmented Bacillus-Subtilis strains and a proposal for Bacillus-Atrophaeus Sp-Nov. Int J Syst Bacteriol. 1989; 39(3):295–300.

Neaman A, Mouele F, Trolard F, Bourrie G. Improved methods for selective dissolution of Mn oxides: Applications for studying trace element associations. Appl Geochem. 2004; 19(6):973–979.

Pardo-Andreu GL, Sanchez-Baldoquin C, Avila-Gonzalez R, Yamamoto ETS, Revilla A, Uyemura SA, Naal Z, Delgado R, Curti C. Interaction of Vimang (Mangifera indica L. extract) with Fe(III) improves its antioxidant and cytoprotecting activity. Pharmacol Res. 2006; 54(5):389–395. [PubMed: 17000117]

Plomp M, Leighton TJ, Wheeler KE, Pitesky ME, Malkin AJ. *Bacillus atrophaeus* outer spore coat assembly and ultrastructure. Langmuir. 2005; 21(23):10710–10716. [PubMed: 16262341]

Rosenberg M. Bacterial adherence to hydrocarbons—A useful technique for studying cell-surface hydrophobicity. FEMS Microbiol Lett. 1984; 22(3):289–295.

Saenz AJ, Petersen CE, Valentine NB, Gantt SL, Jarman KH, Kingsley MT, Wahl KL. Time-of-flight mass spectrometry for replicate bacterial culture analysis. Rapid Commun Mass Spectrom. 1999; 13:1580–1585. [PubMed: 10421900]

Sasaki K, Idachaba MA, Rogers PL. An improved method for cell and spore counts during aerobic cultivation of crystal toxin producing *Bacillus sphaericus*. Biotechnol Tech. 1995; 9:321–326.

Spiro TG, Bargar JR, Sposito G, Tebo BM. Bacteriogenic manganese oxides. Acc Chem Res. 2010; 43:2–9. [PubMed: 19778036]

Sun LP, Zborowski M, Moore LR, Chalmers JJ. Continuous, flow-through immunomagnetic cell sorting in a quadrupole field. Cytometry. 1998; 33(4):469–475. [PubMed: 9845442]

Tobias HJ, Pitesky ME, Fergenson DP, Steele PT, Horn J, Frank M, Gard EE. Following the biochemical and morphological changes of *Bacillus atrophaeus* cells during the sporulation process using bioaerosol mass spectrometry. J Microbiol Methods. 2006; 67:56–63. [PubMed: 16616384]

Valdivia A, Perez-Alvarez S, Aroca-Aguilar JD, Ikuta I, Jordan J. Superoxide dismutases: A physiopharmacological update. J Physiol Biochem. 2009; 65(2):195–208. [PubMed: 19886398]

Zborowski, M.; Chalmers, JJ. Magnetic cell separation. New York: Elsevier Science; 2007. p. 7

Zhang H, Zborowski M, Williams PS, Chalmers JJ. Establishment and implications of a characterization method for magnetic nanoparticles using Cell Tracking Velocimetry and magnetic susceptibility modified solutions. Analyst. 2005; 130:514–527. [PubMed: 15776162]

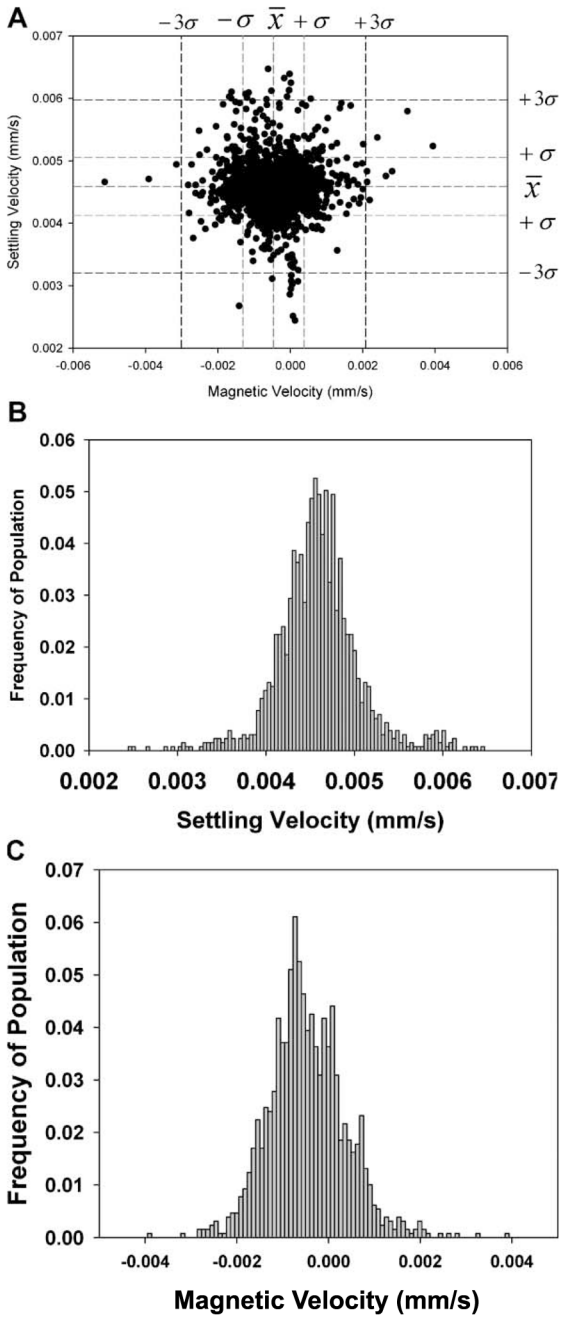

Figure 1.

Dot plot (**A**), histograms of settling velocity (**B**), and magnetic velocity (**C**) for the PSM. In addition, the mean, one and three standard deviations from the mean are presented as dashed lines for the settling and magnetic velocity.

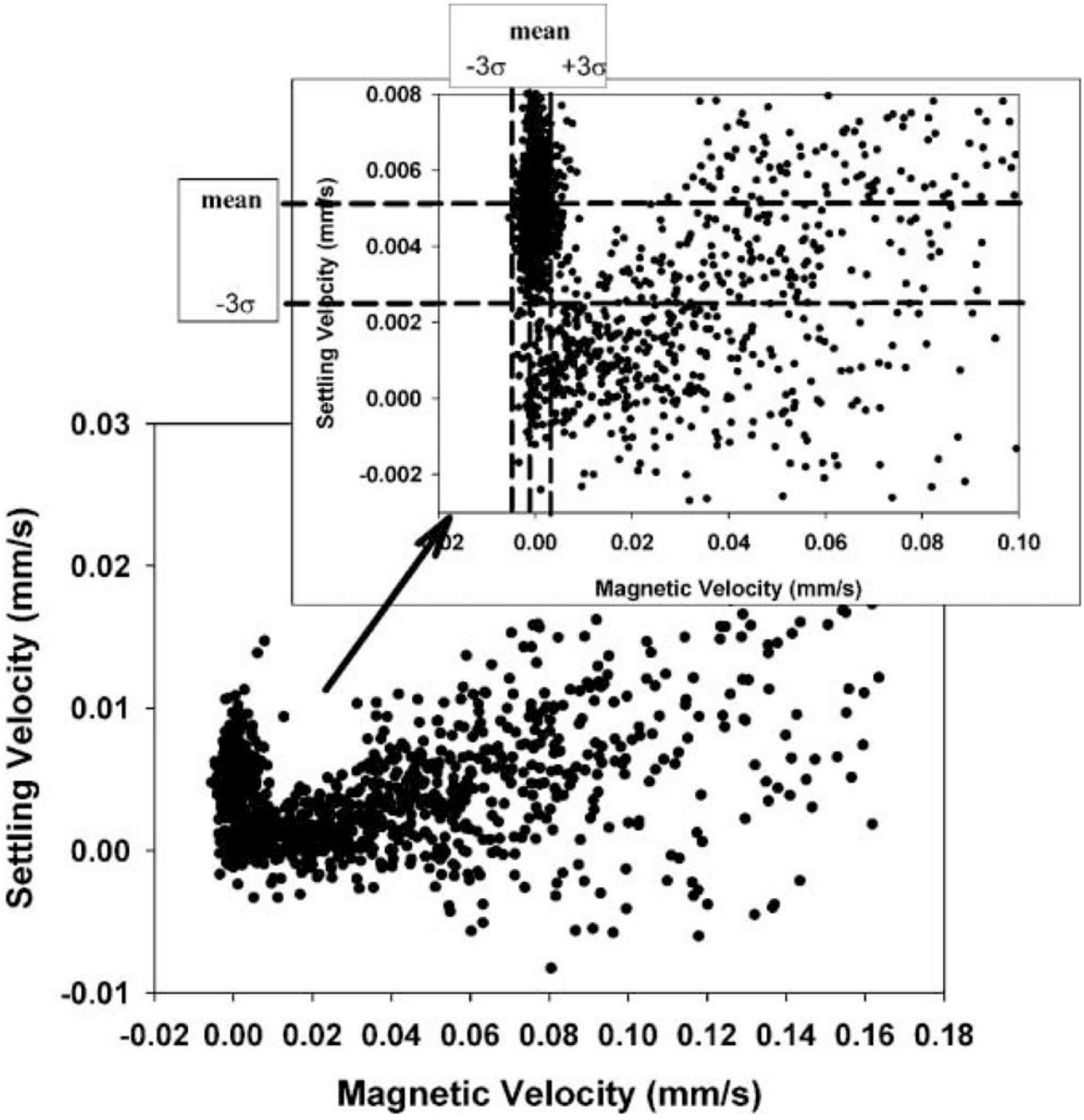

Figure 2.
Dot plots of a full scale, CTV measurement of *Bacillus* spores mixed with 15.3 μm PSM, and inset is an expended scale, dot plot with mean and three standard deviations of the PSM, derived from independent analysis of the PSM.

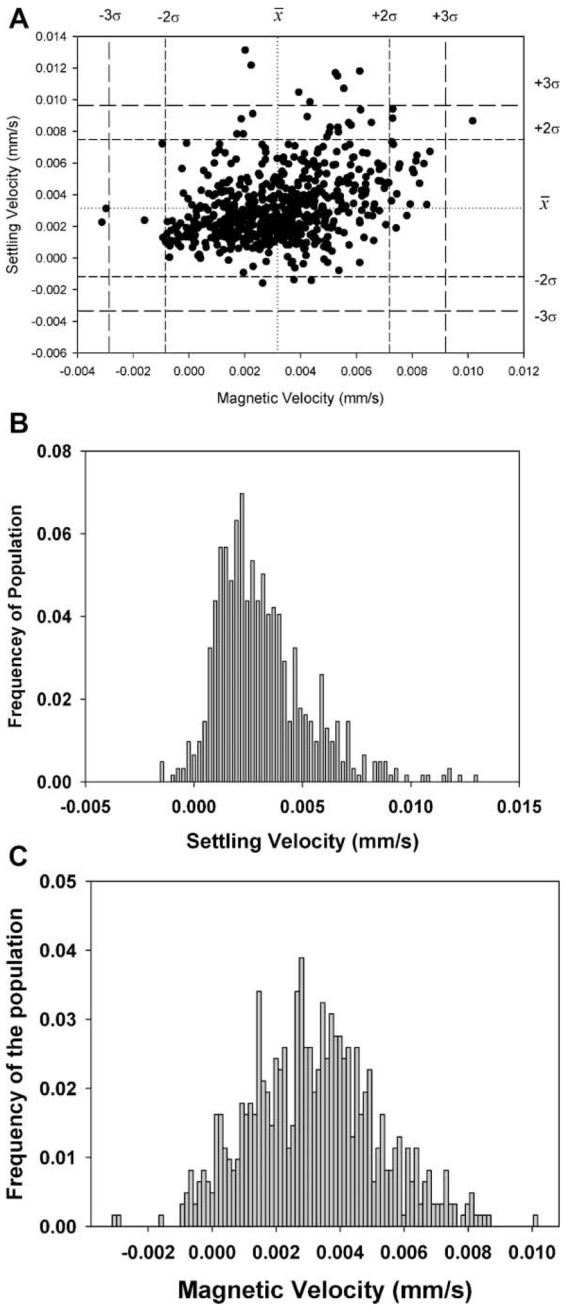

Figure 3.
Representative dot plot (**A**) and histogram of the magnetic velocity (**B** and **C**) histograms of the settling and magnetically induced velocity of the spores not mixed with PSM.

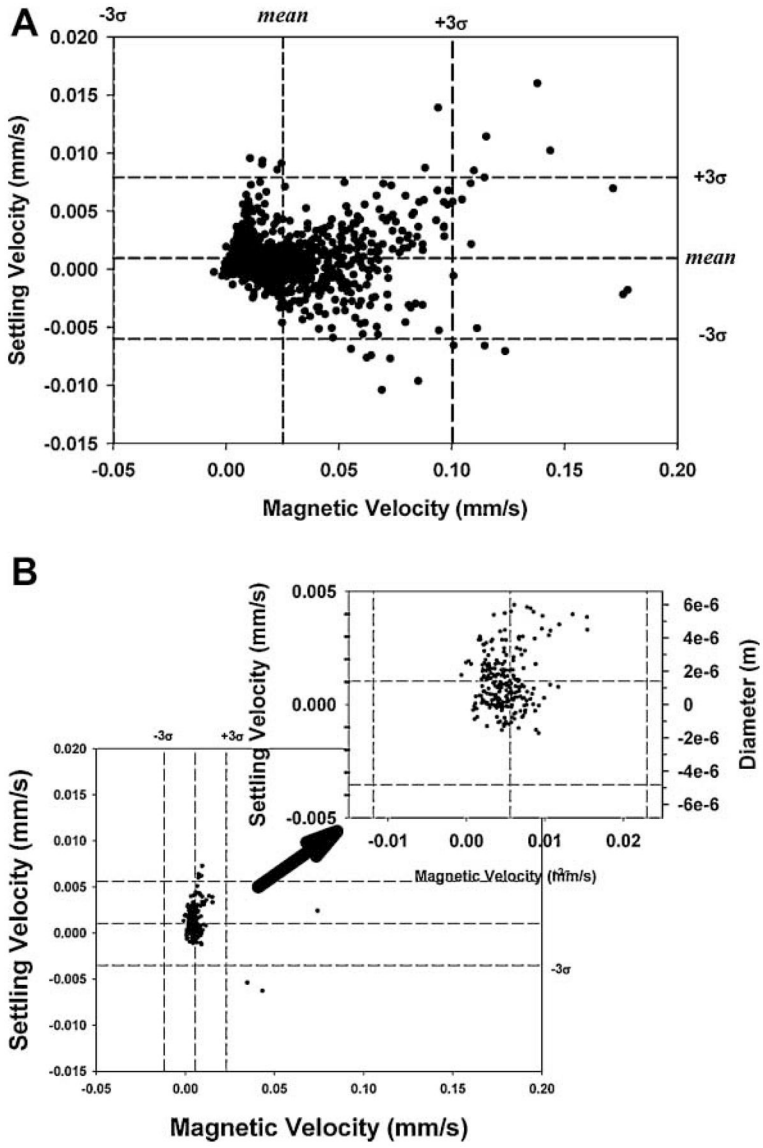

Figure 4.
Settling and magnetic velocity of the spores only in distilled water (A) and in distilled water containing EDTA (B).

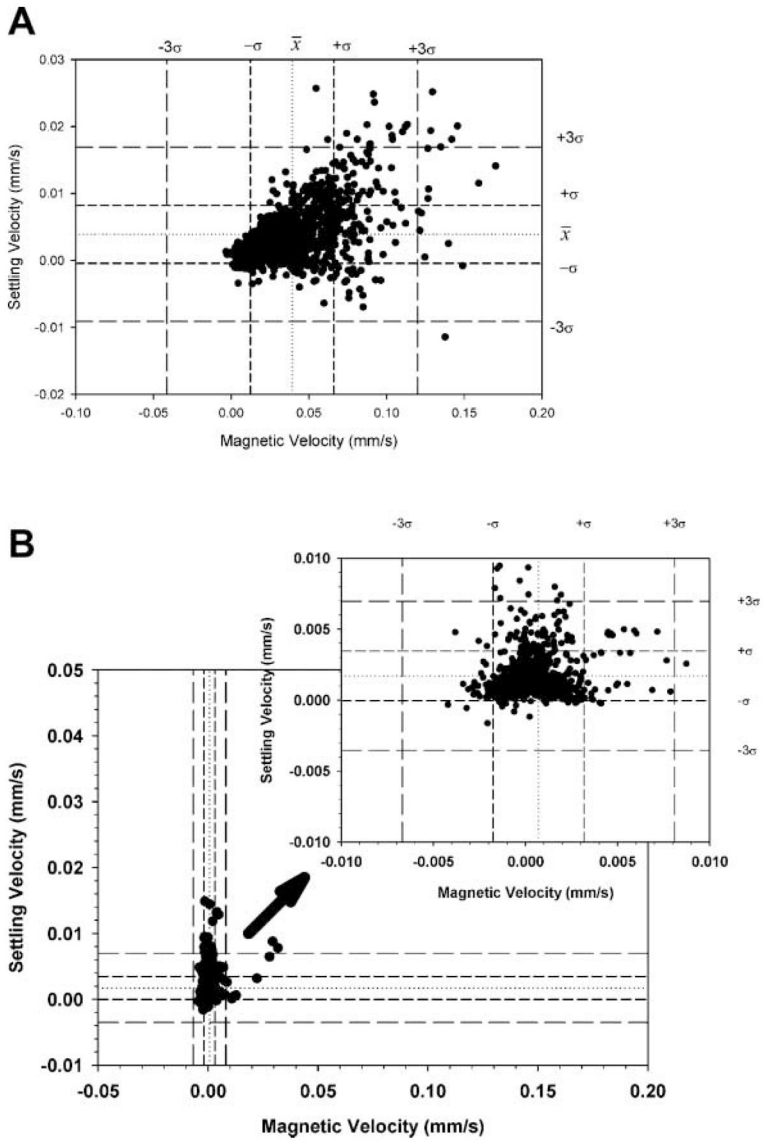

Figure 5.
Settling and magnetic velocity of the spores only in distilled water (A) and after being suspended in a solution of pH 1.0 overnight (B).

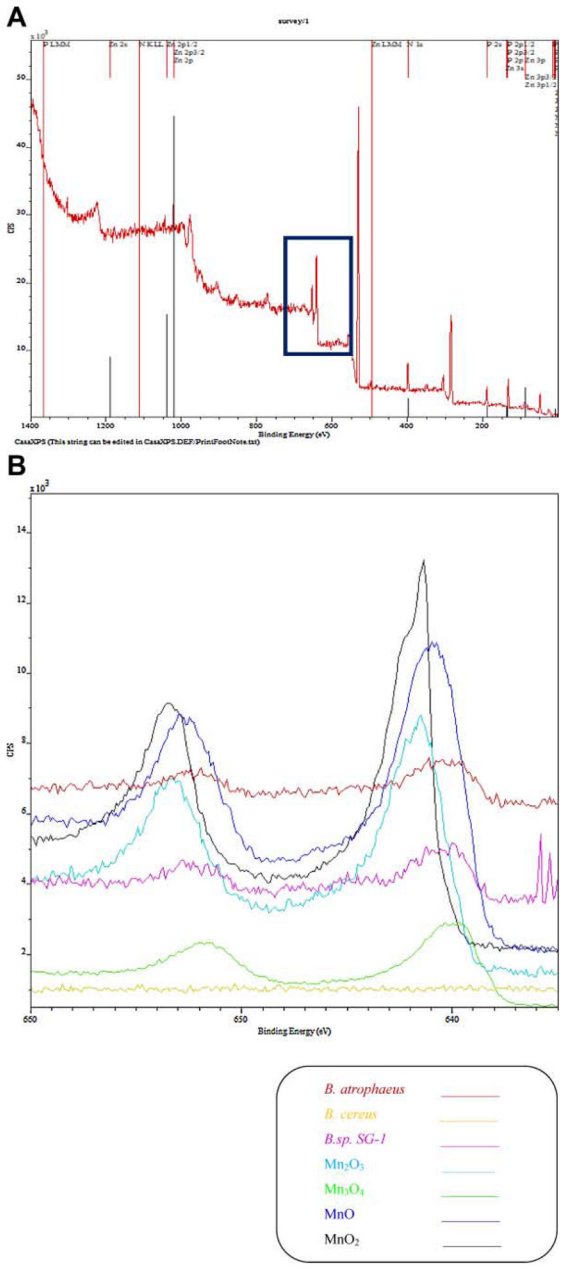

Figure 6.
Full scale XPS spectra, 6A, and enlarged XPS spectra in the region of Mn peaks, for *Bacillus atrophaeus*, *Bacillus cereus*, *Bacillus* sp. SG-1, and Mn oxides standard.

Table I

Magnetic susceptibility parameters of Mn compounds.

Compound	Molecular weight	Specific gravity	Molar magnetic susceptibility $\chi_m \times 10^6$ (cm^3/mol)[a]	Volume magnetic susceptibility (SI)
α Mn	54.938	7.2	529	8.72×10^{-4}
β Mn	54.938	7.2	293	4.82×10^{-4}
MnO (II)	70.94	5.43–5.46	4,850	4.56×10^{-3}
MnO_2 (IV)	86.94	5.026	2,280	1.55×10^{-3}
Mn_2O_3 (III)	157.87	4.5	14,100	5.1×10^{-3}
Mn_3O_4 (III, IV)	228.81	4.856	12,400	3.3×10^{-3}
$MnCl_2$ (II)	161		14,350	
$MnSO_4$–$4H_2O$			14,600	
H_2O	18	1.0	−13.0	-9.04×10^{-6}

[a] In cgs units, for 1 g formula weight.

Table II

CTV analysis of PSM and spores.

Particles	Treatment	Experiment	Mean settling velocity (μm/s)	Mean magnetic velocity (μm/s)	Mean diameter (μm)	Mean magnetic susceptibly × 10^6
PSM	NA	Mean $N = 4$	4.97 ± 0.46	−0.430 ± 0.092	15.3 ± 0.72	−9.28 ± 0.0686
	Mixed with spores	Mean $N = 4$	5.11 ± 0.243	−0.421 ± 0.132		−9.26 ± 0.0746
Bacillus atrophaeus spores	NA	Mean $N = 6$	3.57 ± 1.27	36.9 ± 8.31[a]	5.85 ± 1.12	143 ± 38
	Mixed with PSM	Mean $N = 4$	−2.88 ± 1.21	37.2 ± 7.49	5.06 ± 1.10	186 ± 52
	Detergent effect	Control	0.778	25.7	5.85	437
		EDTA treatment	1.03	5.58	3.08	6.26
		Triton treatment	0.552	7.70	2.25	175
		Tween treatment	0.502	6.81	2.15	170
	pH effect	Control	3.91	39.3	6.0	133
		5.0	4.60	6.86	6.4	19.7
		4.0	4.51	6.73	6.4	19.7
		3.0	3.15	27.3	5.4	115
		2	1.85	0.715	4.1	5.11
		1.2	1.34	1.07	3.96	5.44
		0.6	2.64	3.94	4.26	6.35

[a]Both the permanent and electromagnet CTV was used for these measurements, four with the permanent, and two with the electromagnet. No significant difference was observed.

Table III

Quantification of Mn in different chemical state from XPS.

	Center	Height	FWHM	Area	Proportion[a]	Proportion[b]
Mn^{2+}						
Peak #1	640.179	300	0.9030155	288.3691	0.060191	0.413234
Peak #3	641.2	278.5569	1.6	474.4229	0.099026	
Peak #6	642	236.5623	2	503.6249	0.105122	
Peak #8	642.9	209.9633	0.9824735	219.5819	0.045833	
Peak #14	645	93.44832	2.75	273.5482	0.057098	
Peak #16	647.5	104.6154	1.979269	220.2088	0.045964	
Mn^{3+}						
Peak #2	640.7	673.178	0.806196	644.5823	0.134544	0.380165276
Peak #4	641.4	388.5492	1	460.7613	0.096175	
Peak #7	642.2	335.8108	0.7656146	307.357	0.064155	
Peak #10	643.2	146.7075	1.65	284.4088	0.059365	
Peak #12	644.6	31.37408	3.5	124.2172	0.025928	
Mn^{4+}						
Peak #5	641.9	185.4045	1.5	326.5487	0.06816	0.2066
Peak #9	642.9	135.1923	1.1	176.6936	0.036881	
Peak #11	643.8	117.0724	1.2	166.7105	0.034797	
Peak #13	644.8	75	1.497097	132.3673	0.027629	
Peak #15	645.8	69.9997	2.319403	187.478	0.039132	

[a]Proportion of each peak in that state of Mn.

[b]Proportion of that state of Mn of the total Mn in the sample.

Table IV

ICP-OES analysis of Mn content in spores.

Sample	Mass of (dry) spores (mg)	Concentration of Mn from ICP-MS (μg/mL)	Concentration of Fe from ICP-MS (μg/mL)	Total Mn recovered (g)	Total Fe recovered (g)	Mn (g) per Gram spore	g Mn per cm^3 spore	g Mn per spore cluster
Control	0.00	<0.025	0.2	—	4.1×10^{-6}	—	—	—
Spores, no sonication	5.0	40	1	8.04×10^{-4}	2.01×10^{-5}	0.268	0.322	3.28×10^{-11}
Spores, sonication	5.0	60.5	1.5	1.34×10^{-3}	3.32×10^{-5}	0.160	0.192	1.96×10^{-11}